WEC System Identification and Model Validation

Giorgio Bacelli
Sandia National Labs
Albuquerque, New Mexico, USA

Ryan G. Coe*
Sandia National Labs
Albuquerque, New Mexico, USA

*Corresponding author: rcoe@sandia.gov

1. INTRODUCTION

Numerical models for wave energy converters (WECs) are utilized in a number areas within the design process. These include, but are not limited to, performance assessment, control design, and survival analysis. Thus, the accuracy of such a model is paramount to design of a WEC.

WEC dynamic models can take a number of forms. At the most basic level, the model should capture the rigid-body dynamics based on hydromechanic, kinematic and mechanical considerations. Additional components, capturing power take-off (PTO), realistic mooring systems, and transmission, should ideally be included to produce a so-called "wave-to-wire" model. Here, we focus on the hydrodynamic component of such models.

WEC hydrodynamic models are often based on a radiation/diffraction model (see, e.g., [1]).

$$\left(B(\omega)+B_f+i\left(\omega\left(M+A(\omega)\right)-\frac{K}{\omega}\right)\right)\hat{V}=\hat{H}(\omega)\,\hat{\eta}+\hat{F}_a, \tag{1}$$

Here, $B(\omega)$ and $A(\omega)$ are the frequency dependent radiation damping and added mass respectively. The term B_f accounts for friction effects. The rigid-body mass is given by M. The hydrostatic/gravitational stiffness is linearized as K. Excitation is included via the product of a frequency response function (FRF), $\hat{H}(\omega)$, and the complex wave elevation, $\hat{\eta}$. Input for the actuator/PTO is given by $\hat{F}_a$. We can define the intrinsic impedance of the system as the ratio between the PTO force and the velocity when the excitation force is zero (no waves), that is

$$Z_i(\omega)=\frac{\hat{F}_a}{\hat{V}}=B(\omega)+B_f+i\big(M+A(\omega)-K/\omega\big). \tag{2}$$

This allows Eqn. (1) to be rewritten as

$$\hat{V}=\frac{H(\omega)}{Z_i(\omega)}\,\hat{\eta}+\frac{1}{Z_i(\omega)}\hat{F}_a. \tag{3}$$

Table 1: Model-scale WEC physical parameters.

Parameter	Value
Rigid-body mass (float & slider), m (kg)	858
Displaced volume, $\forall$ (m^3)	0.858
Float radius, r (m)	0.88
Float draft, T (m)	0.53
Water density, ρ (kg/m^3)	1000

The terms in Eqns. (1)-(3) must be defined depending on the particular geometry of the WEC of interest. This is often accomplished using boundary element model (BEM) tools such as WAMIT [2] and NEMOH [3]. Alternatively, and also as a way of validating a model based on BEM, experimental tests can be used to perform a system identification (SID). Procedures for carrying out experimental testing of a WEC in a wave tank and the subsequent data processing to produce a model have been mostly based on the approaches used for testing of ships and offshore structures.

Here, we present an experimental design and SID process that takes advantages of a set of methods widely used for a variety of engineering systems. Some more in-depth investigations and discussions on this process available in [4, 5]. First, a discussion of SID considerations for a WEC is presented. Next, the experimental setup and device studied for this paper are introduced. A specific example of a SID and model validation process is then presented. Finally, a discussion on model formulations

1.1 Experimental setup

A 1/17 model-scale wave tank test was conducted using the point absorber WEC shown in Figure 1 [4, 5]. Relevant physical parameters for this device are listed in Table 1. Testing was performed at the US Naval Surface Warfare Center, Carderock Division (NSWCCD) Maneuvering and Sea Keeping Basin (MASK). A full public dataset from this testing is available at `https://mhkdr.openei.org/submissions/151`.

1.2 Considerations for WEC SID

While many SID processes on WECs have been con-

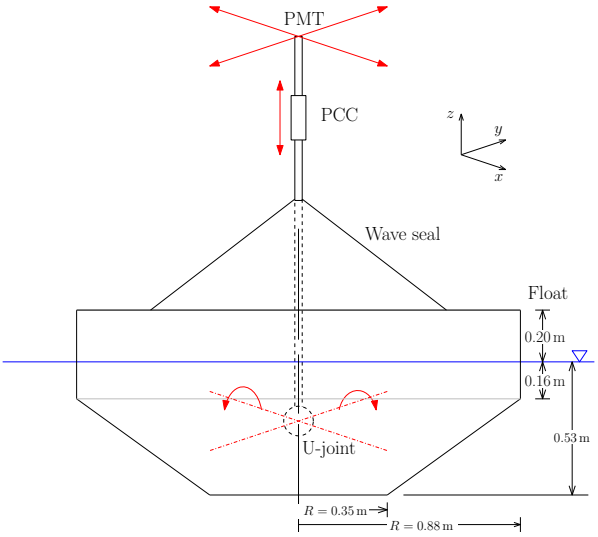

Figure 1: Test device diagram.

ducted using monochromatic waves, as discussed in [4, 5], there are a number of advantages to choosing periodic multi-sine signals for the system input. With the data processing procedures demonstrated in this paper, multi-sine input signals can provide much higher frequency fidelity models in less time than monochromatic tests. Additionally, periodic multi-sine signals can be used to obtain a number of benefits.

- **Smoother wave spectra** - Figure 2 shows a comparison of spectral energy density for two different realizations of the same Bretschneider sea state ($H_s = 0.192\,\text{m}$, $T_p = 4.00\,\text{s}$). One realization uses a psuedo-random wave component phasing to produce a wave train with a 2 hour repeating period. For this test, 30 minutes of that 2 hour period were used to produce a non-repeating wave. The second realization uses a periodic signal. The component phasing is such to produce a wave train with a 5 minute repeat period. For the experiment, this 5 minute signal is repeated three times, to produced a 15 minute experiment duration. The periodic wave provides a fuller/smoother spectrum with fewer dips. Note also that this full spectrum is obtained with half the experiment time required by a pseudo-random approach.
- **Reduced spectral leakage** - When taking the discrete Fourier transform (DFT) of a signal with a non-integer number of periods, spectral leakage can occur. Periodic multi-sine input signals in testing, allow the DFT to be cleanly obtained for both the input (i.e. from wave probes) and for the output (i.e. device response) without the use of windowing.
- **Increased signal-to-noise ratio** - By utilizing multiple periods of the same signal, random noise effects in the response can be reduced.
- **Nonlinearity detection** - Energy input at a given frequency in a linear time-invariant (LTI) system can only excite a response at that same frequency. Thus, one can identify nonlinear effects in a system response by finding harmonics outside of the frequencies in the excitation signal.

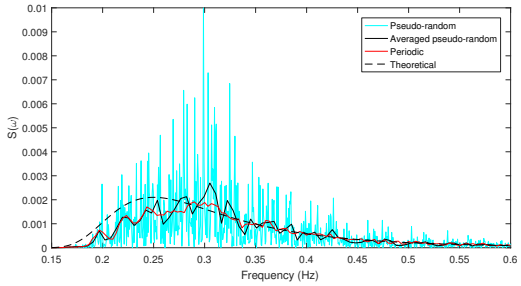

Figure 2: Spectral density of pseudo-random (2 hour repeat, 30 minute wave) and periodic (5 minute repeat, 15 minute wave) Bretschneider ($H_s = 0.192\,\text{m}$, $T_p = 4.00\,\text{s}$) wave realizations.

Figure 3 illustrates the process for constructing a radiation/diffraction model for a WEC. This process includes two experimental tests:

- **Forced oscillation test** - The device is excited using its actuator(s) in calm water (only damping input to wavemakers). The device should be driven with a force control, using a multi-sine input signal, such as band-limited flat (white) spectrum. The ratio of the input force, $\hat{F}(\omega)$, and the resulting velocity, $\hat{V}(\omega)$, can then be taken to give the intrinsic impedance, $\hat{Z}_i(\omega)$.
- **Diffraction test** - The device is locked in place and subjected to wave input. Wave input should be a band-limited multi-sine signal. While idealized ocean spectra (e.g. Bretschneider) are acceptable, flatter spectra are more desirable. White (flat) spectra waves have a tendency to break, because the wave steepness increases as the frequency increases; pink spectra, however, where the amplitude of each component is inversely proportional to the frequency, can be used instead to prevent wave breaking. The force required to prohibit the motion of the device is measured. The excitation FRF, $\hat{H}(\omega)$ can be obtained by taking the ratio of the excitation (locking) force, $\hat{F}_{ex}(\omega)$, and the wave elevation, $\hat{\eta}(\omega)$.

By combining these two paths, we can obtain the model illustrated by the block diagram in Figure 3.

Note that the typical approach used for wave tank testing of a WEC assesses WEC performance by running a test matrix of waves and constant PTO dampings; this procedure is used to produce power curves. The issue with this approach, as discussed in [5], is that tests conducted while applying a feedback control have a limited utility for SID. The approach followed in this study produces a model of the WEC system without any correlation to a specific PTO damping. This approach is more general, as it produces a model of the WEC system which can be used for producing power curves as

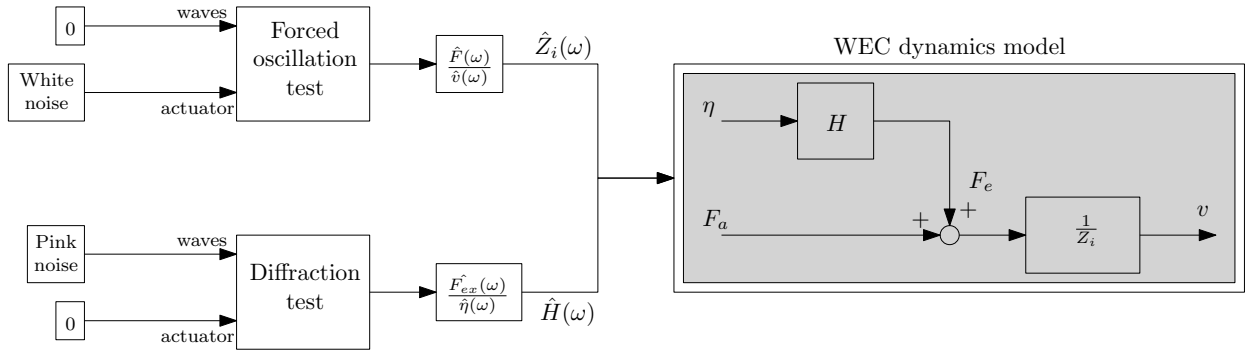

Figure 3: Diagram of SID process for radiation/diffraction model of a WEC.

well as many more general applications, such as control design.

2. RADIATION/DIFFRACTION MODEL CONSTRUCTION

In this section, we demonstrate the SID process discussed in Section 1.2 and perform a validation test on the resulting model. Figure 4 shows the intrinsic impedance model. For comparison with the empirical model identified in this study ("experimental" in Figure 4), a numerically based model produced with WAMIT is also shown. Additionally, a frequency-averaged version of the empirical model ("experimental (smoothed)" in Figure 4) is also shown.

The excitation model is shown in Figure 5. Here, a number of empirical models ("Staff1," "Staff2," ...) are shown with a model from WAMIT. The different empirical models use different wave sensors for the wave elevation, $\hat{\eta}(\omega)$. Note that, as discussed in [4, 5], these wave elevations are not taken at the location of the device, as is often the case. Instead, each of these sensors is taken at a different location; thus the phases shown in the Figure 5 have been shifted to overlap.

3. MODEL VALIDATION

For validation, a third data set, not used in any of the previous SID work, is consider. For this experimental test, the device was excited with both the actuator and waves. the waves were given by a Bretschneider spectrum with $H_s = 0.155\,\text{m}$ and $T_p = 2.39\,\text{s}$. An uncorrelated pink multisine signal was used for the actuator. The velocity in the experimental test was measured and then compared with the velocity predicted by the model identified in Section 2. The results of this comparison are shown in Figure 6. To provide a quantitative measure of model performance, the normalized root mean square error (NRMSE) between the measured and predicted velocity was determined. For this case, the model has a 71.6% fit ($1 - \text{NRMSE} = 0.716$).

4. MULTIPLE-INPUT SINGLE-OUTPUT MODEL

In an alternative approach, the WEC can also be modeled as a Multiple-Input Single-Output (MISO) system, where the inputs are the force F_a and the wave elevation measured by the wave probe η^{tot}, and the output is the velocity v, as depicted in Figure 7. MISO models are commonly used and extensive literature is available in both control design [6] and SID [7, 8]. The SID procedure for the MISO model is carried out in "open loop" by applying independent signals to both inputs; in particular, pink multi-sines with random phases can be used for the wave elevation and the force. The mathematical model for the MISO structure is

$$v = G_1 F_a + G_2 \eta^{tot}. \tag{4}$$

Figure 8 shows the FRFs of the two blocks composing the MISO and the FRFs obtained from the radiation/diffraction approach; it can be seen that there is a good agreement between the two approaches.

5. DISCUSSION

The model formulation considered in this paper is that which is most commonly used for WECs. Note however that alternative approaches have been considered and can provide a number of advantages. While the radiation/diffraction formulation is the most familiar, one must consider the real purpose for developing a model. Specifically, models which use pressure to incorporate the excitation phenomena have been shown to provide better accuracy than those based on wave elevation [4, 5]. These pressure-based models also have a number of potential benefits for implementation, in that they are based more directly on the causal input to the dynamic system.

6. CONCLUSION

This study considered the SID process for a WEC. The experimental design and data processing practices best-suited to the efficient development of an accurate model were discussed. Using data from a model-scale wave tank test, an empirical model was identified for a single body point absorber. This model was validated and shown to have good agreement with the actual system.

7. ACKNOWLEDGEMENTS

This work was funded by the U.S. Department of Energy's Water Power Technologies Office. Sandia National Laboratories is a multi-mission laboratory managed and operated by Sandia Corporation, a wholly

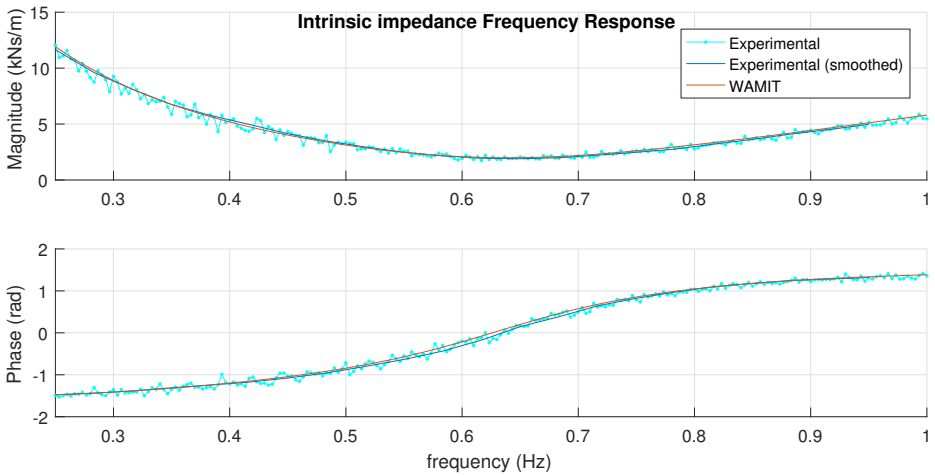

Figure 4: Magnitude and phase of intrinsic impedance, $\hat{Z}_i(\omega)$, for a white multi-sine input force. The estimated linear friction is $B_f = 460\,\mathbf{Ns/m}$.

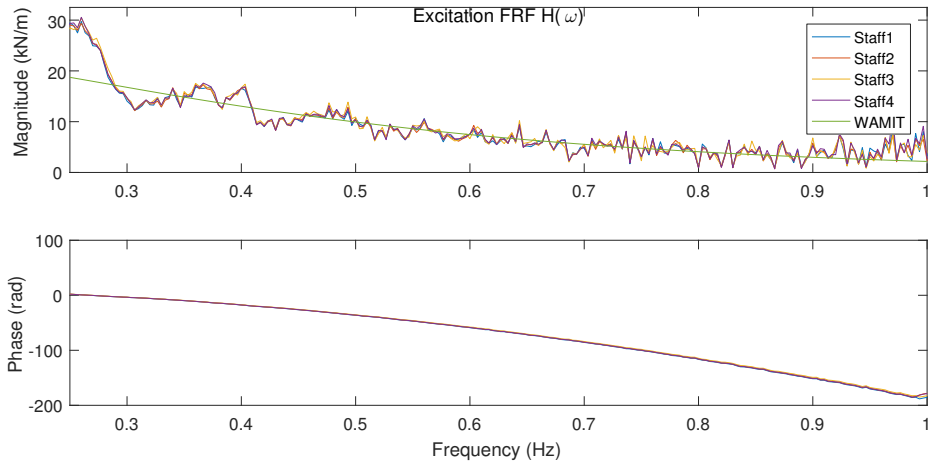

Figure 5: Excitation force FRFs, $\hat{H}(\omega)$, calculated using signals from multiple wave probes ("Staff1," "Staff2," ...).

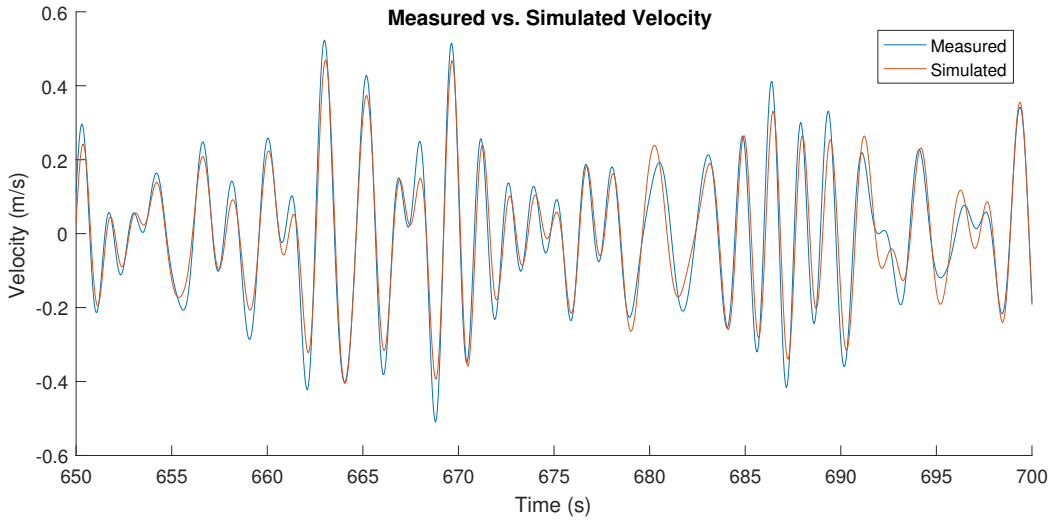

Figure 6: Radiation/diffraction model validation: time series detail of measured (experimental) velocity compared to simulated velocity ($1 - \mathbf{NRMSE} = 0.716$).

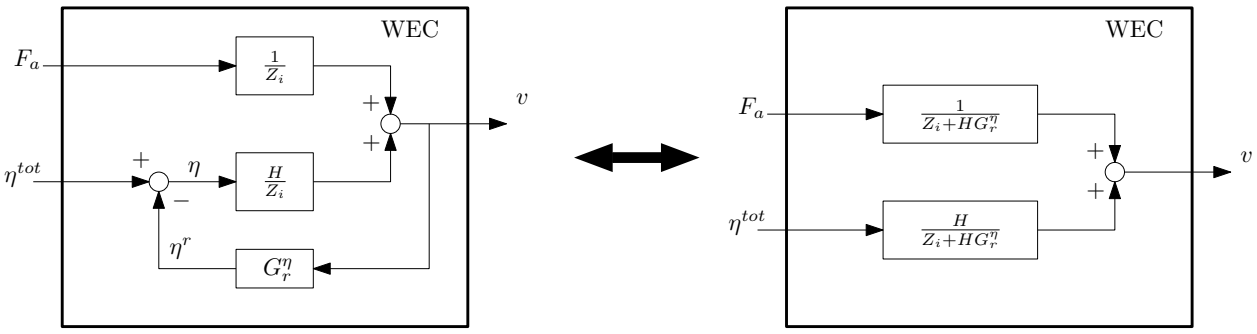

Figure 7: MISO block diagram

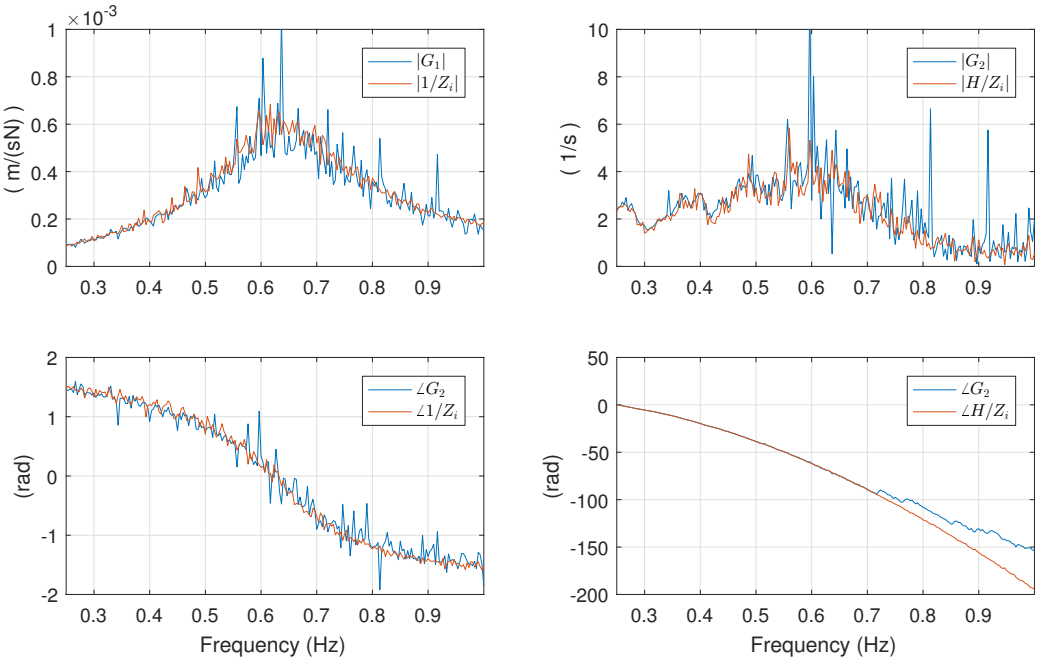

Figure 8: Comparison of FRFs for dual SISO and MISO models

owned subsidiary of Lockheed Martin Corporation, for the U.S. Department of Energy's National Nuclear Security Administration under contract DE-AC04-94AL85000.

8. REFERENCES

[1] Falnes, J., 2002. *Ocean Waves and Oscillating Systems*. Cambridge University Press, Cambridge; New York.

[2] WAMIT, 2012. *WAMIT User Manual*, 7 ed. Chestnut Hill, MA.

[3] Babarit, A., and Delhommeau, G., 2015. "Theoretical and numerical aspects of the open source bem solver nemoh". In 11th European Wave and Tidal Energy Conference (EWTEC2015).

[4] Coe, R. G., Bacelli, G., Patterson, D., and Wilson, D. G., 2016. Advanced WEC Dynamics & Controls FY16 testing report. Tech. Rep. SAND2016-10094, Sandia National Labs, Albuquerque, NM, October.

[5] Bacelli, G., Coe, R. G., Patterson, D., and Wilson, D. G., 2017. "System identification of a heaving point absorber: design of experiment and device modeling". *Energies (in-press)*.

[6] Ogata, K., 2002. *Modern Control Engineering*. Prentice Hall.

[7] Ljung, L., 1999. *System identification - Theory for the User*. Prentice-Hall.

[8] Pintelon, R., and Schoukens, J., 2012. *System identification: A frequency domain approach*. John Wiley & Sons.